

Deswelling Microgel Particles Using Hydrostatic Pressure

Juan-Jose Lietor-Santos,[†] Benjamin Sierra-Martin,[†] Ronny Vavrin,[§] Zhibing Hu,[‡]
Urs Gasser,^{§,||} and Alberto Fernandez-Nieves*,[†]

[†]School of Physics, Georgia Institute of Technology, Atlanta, Georgia 30332, [‡]University of North Texas, Denton, Texas 76203, [§]Laboratory for Neutron Scattering, ETH Zurich, and Paul Scherrer Institute, 5232 Villigen PSI, Switzerland, and ^{||}Adolphe Merkle Institut, University of Fribourg, P.O. Box 209, 1723 Marly 1, Switzerland

Received May 15, 2009; Revised Manuscript Received June 9, 2009

ABSTRACT: We report on the use of hydrostatic pressure, P , to deswell thermosensitive poly(N -isopropylacrylamide) (pNIPAM) microgels and show that it can affect the polymer–solvent mixing as much as temperature, which is the traditional variable used to deswell pNIPAM particles. Interestingly, the microgel volume changes more gradually with pressure than it does with temperature. By comparing the pressure and temperature induced deswelling, we obtain the pressure dependence of the Flory solvency parameter, χ ; it increases with P , indicating that pressure decreases the polymer–solvent miscibility. We interpret this increase in terms of the entropy change, ΔS , when a polymer–solvent contact is broken to form a solvent–solvent contact and find that $|\Delta S|$ also increases with P , consistent with previous experimental results with polymers and other gels. Hydrostatic pressure thus changes the entropic contribution of mixing, causing χ to increase and ultimately leading to particle deswelling.

Introduction

The swelling of polymeric gels, which are cross-linked networks that can undergo dramatic volume transitions in response to environmental changes, is one of the central issues in polymer physics.^{1,2} Flory studied the volume transition of the gel by considering the balance between the osmotic pressure arising from the polymer–solvent mixing and the osmotic pressure arising from the network elasticity.³ Some years later, Tanaka reported the synthesis of the first poly(acrylamide) gel in a mixture of solvents, which successfully collapsed upon changes in temperature.⁴ This volume transition was easily explained in terms of Flory's theory by considering a change in the solubility parameter, often referred to as the Flory parameter, χ , accounting for the affinity between the polymer and the solvent. At low temperatures, the mixing parameter is small and the polymer–solvent contacts are favored over the solvent–solvent contacts. As a result, the particle is swollen. By contrast, at high temperatures, the Flory parameter is large and the particle is deswollen. Unfortunately, the time associated to these volume changes is typically very large,^{5–7} preventing in many cases a more extended use in technological applications. Nevertheless, several methods have addressed this issue and fast responsive gels based, for example, on comb-type grafted hydrogels^{8–10} and surfactant-grafted hydrogels^{11,12} have been successfully made. An alternative to these approaches is to reduce the polymer gel size by producing microgels.

Microgel particles are gels in the colloidal domain.^{13,14} As a result, they also swell and deswell in response to environmental changes, but interestingly, they do so much faster than macroscopic gels.^{15,16} Furthermore, since microgels are immersed in a solvent, the macroscopic behavior of the suspension also depends on the particle–particle interactions and thus on the resultant phase behavior. Microgel suspensions are, in this sense, richer

systems than their macroscopic counterparts. They were first synthesized by Pelton and Chibante using an emulsion polymerization method¹⁷ and since then, they have been extensively used in various applications,^{18–20} including artificial muscle fabrication,²¹ drug delivery,^{22,23} optical switching,^{24,25} microfluidic devices,²⁶ water purification technologies²⁷ and oil recovery.^{28–30} From a more fundamental point of view they have been used to address basic questions in condensed matter physics, including crystallization,³¹ melting,³² the glass transition,^{33,34} and geometrical frustration.³⁵ In these applications, microgels are treated as hard spheres with an externally tunable volume; this provides an elegant way to tune the suspension volume fraction, which is the relevant thermodynamic variable for these model systems.

The most widely used microgel particle is based on poly(N -isopropylacrylamide) (pNIPAM), which is a thermosensitive polymer that allows particle-size tunability with temperature.^{36–38} Although simple to achieve, a change in temperature can sometimes require long equilibration times and often this happens heterogeneously throughout the sample and in a hardly controlled manner; these effects can severely affect the suspension behavior in undesired ways. In this context, an alternative to temperature is provided by hydrostatic pressure, which is also known to change the polymer–solvent mixing of pNIPAM gels.^{39–43} The influence of pressure over the swelling of microgel particles, however, has never been explored, despite the fact that pressure changes can be achieved in very short times, as they propagate at the speed of sound of the material, and occur homogeneously throughout the sample. The major drawback is, however, the need of a pressure chamber, which often requires substantial technical efforts.⁴⁴

In this work, we measure the size dependence of pNIPAM-based particles as a function of temperature and hydrostatic pressure and show that either of them can be used to effectively change the particle volume. Interestingly, with pressure, deswelling occurs in a more continuous manner, as compared to temperature; this can be useful if fine control of the suspension volume fraction is desired. From the pressure and temperature

*Corresponding author. Telephone: + 14043853667. Fax +14043853681. E-mail: alberto.fernandez@physics.gatech.edu.

swelling curves, and using the classical Flory theory for polymer gels, we obtain the pressure dependence of the Flory parameter; it increases with pressure indicating a progressively poorer mixing of the polymer and the solvent. We suggest that this dependence reflects the raise with pressure of the entropy change associated to the polymer–solvent mixing, consistent with what is experimentally found for polymers⁴⁵ and gels that deswell with increasing temperature⁴⁶ or salt.⁴⁷ Our results provide a controlled way to tune the microgel size and thus the suspension volume fraction by tuning of the polymer–solvent mixing; this could be relevant for fundamental studies, where microgel suspensions are used as model colloidal suspensions with tunable volume fraction. In addition, understanding how pressure affects the microgel swelling behavior can also have technological implications, for instance, in oil extraction processes, where the pressure in the oil cavity can be several orders of magnitude greater than the pressure on the ground.

Experimental Section

Microgel Synthesis. Microgel particles are based on the synthesis of *N*-isopropylacrylamide copolymerized with allylamine and a cross-linker. The particles are synthesized using an emulsion polymerization method where 3.845 g of NIPAM monomer, 0.20 g (10% molar ratio) of allylamine monomer, 0.15 g (2.5% molar ratio) of methylenebis(acrylamide) cross-linker, 0.70 g of the surfactant sodium dodecyl sulfate, and 230 mL of deionized water are mixed in a reactor. All the materials are provided by Aldrich with analytical grade of purity and used without further purification. The solution is first heated to 60 °C under an inert atmosphere with constant nitrogen bubbling and kept at this temperature for 40 min. Then, 0.155 g of potassium persulfate, dissolved in 20 mL of deionized water, is added to initiate the reaction, which is carried out for 5 h at a constant temperature of 60 °C. After cooling the reaction products to room temperature, the final dispersion is filtrated and then exhaustively dialyzed against ultrapure water. The system is then freeze-dried and redispersed in D₂O.

Light Scattering Experiments under Controlled Hydrostatic Pressure. Measurements with pressure are performed using a high pressure cell, which consists of a sample container between two parallel sapphire windows and is designed for a small angle neutron scattering line at the Paul Scherrer Institute.⁴⁴ The pressure is applied using hydraulic oil and a pressure generator. As a result of the particular arrangement of our setup, we use an in-house apparatus to perform dynamic light scattering experiments. It consists of a vertically polarized He–Ne laser operating at a wavelength of 632.8 nm that impinges on the sample. The scattered light is collected at a scattering angle of 135° in a single mode fiber after passing a vertical polarizer, and is splitted into two beams, using a fiber beam splitter, and coupled to two avalanche photodiodes (APDs), which we use as detectors. The signal in the two detectors is cross-correlated in a two channel correlator to effectively avoid the after-pulsing of the APDs.⁴⁸ In this way, we measure the intensity correlation function, which we transform into the field correlation function using the Siegert relation.⁴⁹ Since our experiments are based on dilute samples, this function is well fitted by a single exponential with a characteristic relaxation frequency that depends on the diffusion coefficient, which we relate to the particle size using the Stokes–Einstein relation.⁴⁹ We perform these experiments at different temperatures and pressures to obtain how the microgel size depends on both variables.

Typical particle size distributions and temperature-dependent hydrodynamic radii for pNIPAM-allylamine particles identical to those used in this work have been previously reported.⁵⁰ Consistent with these measurements, the polydispersity index of our particles is less than 1.01. As a result, the particle size deviation from its mean value is less than 10%.

Furthermore, we find that the suspensions crystallize above a certain particle volume fraction, also consistent with the narrow size distribution experimentally found. All particle sizes are the result of three independent measurements and each of these is the average of at least three consecutive measurements. For the size-temperature determinations, we always allowed time for equilibration of the temperature within the sample (~30 min). For the size-pressure experiments this was not needed due to the almost instantaneous pressure equilibration times. We nevertheless confirmed that from immediately after changing the pressure, up to ~2 h later, the particle size remained unchanged.

We note that we work at a solution pH of around 7. Since the pK_a of poly(allylamine) is ~8.8,⁵¹ we expect some of the amino groups in this molecule to be charged. However, due to the hydrophilic nature of allylamine, these groups are preferentially incorporated in the periphery of the particle during the polymerization process and do not notably affect the swelling behavior. Consistent with this, previous measurements identified no significant difference in the temperature dependence of the particle size for pure pNIPAM and pNIPAM-allylamine microgels.⁵⁰ In particular, the size ratio between swollen and deswollen phases is identical for both systems, indicating that any possible reaction between the cross-linker and allylamine does not significantly change the number of chains in the microgel particles, which we can safely estimate using the concentration of cross-linker employed in the particle synthesis. The presence of allylamine slightly increases the hydrophilicity of the overall microgel, promoting a better mixing with the solvent.⁵⁰ In addition, it provides binding sites for possible second-step reactions⁵⁰ or functionalizations of the particles, for instance with fluorescein or rhodamine.⁵²

Results and Discussion

Temperature-Induced Volume Transition. The particle radius, a , decreases with temperature, T , as shown in Figure 1; this is the expected behavior for a pNIPAM-based microgel, which is characterized by a lower critical solution temperature (LCST).^{53–56} As the temperature increases, the microgel gradually shrinks toward a final deswollen radius of $a_0 \approx 60$ nm, which is achieved for $T \geq 312$ K. The transition temperature for our particles, defined as the temperature corresponding to the maximum slope in the size–temperature curve, is 307 K, which is consistent with what is measured for most pNIPAM-based systems in D₂O.^{57–59}

To account for this temperature dependence, we use Flory's theory for the swelling of polymer gels. In this context, equilibrium is achieved when the chemical potential

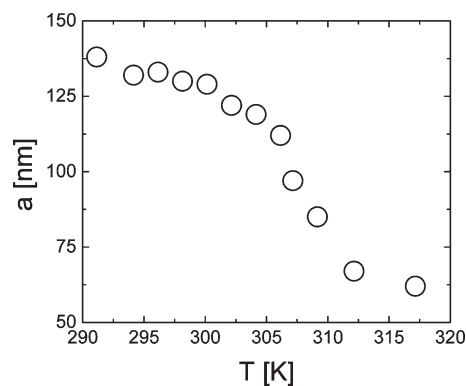


Figure 1. Particle radius of pNIPAM-allylamine microgels in D₂O as a function of temperature. The particle deswells as temperature increases, as expected for a system with a LCST. The size at high temperature is taken as the deswollen size, $a_0 = 60$ nm.

Table 1. Results of the Size–Temperature Fits for Different ϕ_0 ^a

| ϕ_0 | 0.6 | 0.65 | 0.7 | 0.75 | 0.8 | 0.85 | 0.9 | 0.95 |
|------------------------------|-------|-------|-------|--------|---------------|---------------|--------|--------|
| N_c | 31350 | 48838 | 75128 | 114780 | 175220 | 269180 | 420080 | 675730 |
| Θ (K) | 316 | 316 | 315 | 315 | 315 | 314 | 314 | 314 |
| A | −1.9 | −2.6 | −3.5 | −4.7 | −6.4 | −8.8 | −12.4 | −18.2 |
| χ_1 | 0.56 | 0.6 | 0.63 | 0.68 | 0.72 | 0.78 | 0.84 | 0.91 |
| ΔS (10^{-23} J/K) | −3.36 | −4.27 | −5.49 | −7.16 | −9.49 | −12.8 | −17.8 | −25.9 |
| ΔH (10^{-20} J) | −0.83 | −1.13 | −1.52 | −2.04 | −2.77 | −3.82 | −5.39 | −7.89 |

^aThe bold entries correspond to the best fits.

of the solvent inside and outside the microgel become equal or, equivalently, when the net osmotic pressure is equal to zero. For a neutral microgel, the osmotic pressure arises from two major contributions, the mixing of the polymer and the solvent, and the elasticity resulting from cross-linking the polymer to form the polymer network.

The osmotic pressure due to mixing can be written as^{2,3}

$$\Pi_{\text{mix}} = -\frac{N_A k_B T}{v_s} [\phi + \ln(1 - \phi) + \chi \phi^2] \quad (1)$$

with N_A the Avogadro number, k_B the Boltzmann constant, $v_s = 1.81 \times 10^{-5} \text{ m}^3$ the molar volume of D_2O , which is our solvent, χ the Flory parameter that accounts for the solubility of the polymer in the solvent, and ϕ the polymer volume fraction in the particle. For a microgel that swells isotropically³

$$\phi/\phi_0 = (a_0/a)^3 \quad (2)$$

where we choose a_0 and ϕ_0 as the particle size and volume fraction in the deswollen state.

The elastic contribution to the net osmotic pressure is given by^{2,3}

$$\Pi_e = \frac{N_c k_B T}{V_0} \left[\left(\frac{\phi}{2\phi_0} \right) - \left(\frac{\phi}{\phi_0} \right)^{1/3} \right] \quad (3)$$

where N_c is the number of chains in a microgel particle and $V_0 = 4\pi a_0^3/3$.

These two contributions balance each other in equilibrium, where the net osmotic pressure is zero:

$$\Pi_{\text{total}} = \Pi_{\text{mix}} + \Pi_e = 0 \quad (4)$$

This expression provides the equation of state for our microgel particles. As a result, the equilibrium size of a microgel is determined by χ , provided the rest of the variables remain constant along the volume transition. This parameter reflects the affinity of the polymer for the particular solvent; it depends on the free energy change due to the replacement of a solvent–polymer contact by a solvent–solvent contact^{2,3,60}

$$\chi = \frac{\Delta H - T\Delta S}{k_B T} = \frac{1}{2} - A \left(1 - \frac{\Theta}{T} \right) \quad (5)$$

where ΔS and ΔH are the corresponding entropic and enthalpic changes associated with this process, $A = (2\Delta S + k_B)/2k_B$ and $\Theta = 2\Delta H/(2\Delta S + k_B)$ is the so-called Θ -temperature of the polymer–solvent system; for $T = \Theta$, $\chi = 0.5$ and the second virial coefficient of the mixture becomes 0.⁶¹ The temperature dependence of the microgel size is accounted for through the temperature dependence of χ . However, experimentally it has been found that χ also depends on polymer concentration; the exact dependence changes from one system to another, but it is usually

expressed in terms of a linear expansion with polymer volume fraction:⁶⁰

$$\chi = \chi_0 + \chi_1 \phi + \chi_2 \phi^2 + \dots \quad (6)$$

Here χ_0 is the mixing parameter for $\phi = 0$, as defined in eq 5, and χ_i are the coefficients that multiply the i th power of ϕ , which are assumed to be temperature-independent.

By introducing eq 6 into eq 4, we obtain an explicit equation of state relating the temperature with the polymer volume fraction

$$T\Pi=0 = \frac{A\phi^2\Theta}{\frac{v_s N_c}{N_A V_0} \left[\left(\frac{\phi}{2\phi_0} \right) - \left(\frac{\phi}{\phi_0} \right)^{1/3} \right] - \phi - \ln(1 - \phi) + \left(A - \frac{1}{2} \right) \phi^2 - (\chi_1 \phi + \chi_2 \phi^2 + \dots) \phi^2} \quad (7)$$

which we use to fit our data, using eq 2 to relate ϕ to the particle radius. Since the volume fraction in the deswollen state is unknown, we perform different fits for different values of ϕ_0 , leaving N_c , A , Θ , χ_0 , and χ_1 as free parameters, using the chi-square-criterion to quantitatively compare the quality of the different fits.⁶² We find that for the same ϕ_0 and irrespective of the values of the remaining parameters, chi-square is considerably reduced if a linear dependence is used between χ and the polymer volume fraction; we thus set $\chi_2 = 0$ and use $\chi = \chi_0 + \chi_1 \phi$. Within this approximation, the chi-square values we obtain for the different fits are similar, but the resultant values of the free parameters vary considerably, as shown in Table 1, where we show the results for N_c , A , Θ , and χ_1 , for different values of ϕ_0 . We can compare these results with known values of these parameters. For instance, the number of chains per particle can be estimated from the synthesis by considering that each cross-linker molecule connects two chains. As a result: $N_c = 2N_A V_0 c$, with c the molar concentration of the cross-linker; we obtain $N_c \approx 2.5 \times 10^5$, which is close to the values obtained in the fits for $\phi_0 = 0.8$ and $\phi_0 = 0.85$. In this case, the values of χ_1 , ΔH , and ΔS are also consistent with previously reported values for pNIPAM macroscopic gels⁶⁰ and microgels.^{47,58,63} We thus conclude that a value of $\phi_0 = 0.8$ or $\phi_0 = 0.85$ not only provides a reasonable fit to the data, as shown in Figure 2a, but also results in values for the free parameters which are in agreement with what is expected from the microgel synthesis and with previous experimental results.

From the experimental size–temperature dependence, we can use eqs 5 and 6 together with the values of the fitting parameters to obtain the temperature dependence of the Flory parameter, as shown in Figure 2b, where χ is plotted as a function of $1/T$. At low temperatures, the contribution from ϕ in eq 6 becomes almost negligible, as the particles are highly swollen, and the polymer volume fraction is small. As a result, χ scales linearly with $1/T$, as shown by the line in Figure 2b and consistent with what is expected from eq 5. By contrast, for temperatures above the transition temperature, the particle size has appreciably dropped and the ϕ -dependence of the mixing parameter becomes relevant. As a result, the $\chi - 1/T$

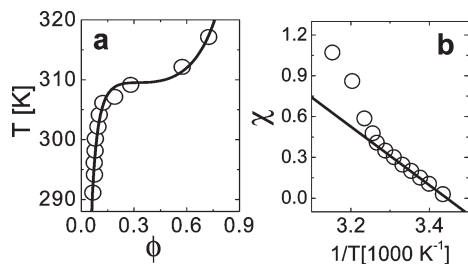


Figure 2. (a) Temperature-induced volume transition of the pNIPAM-allylamine microgel particles in D₂O. The solid line corresponds to the best fit with $\phi_0 = 0.8$, $N_c = 1.75 \times 10^5$, $A = -6.4$, $\Theta = 315$ K, and $\chi_1 = 0.72$. (b) Dependence of the Flory solvency parameter with inverse temperature. As expected from eqs 5 and 6 for high values of $1/T$ (low temperatures), where ϕ is low, the mixing parameter is inversely proportional to T .

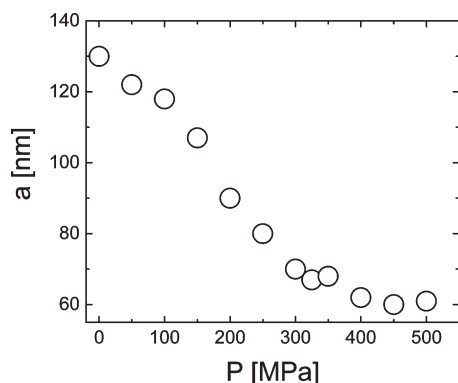


Figure 3. Particle radius of pNIPAM-allylamine microgels in D₂O as a function of pressure. The particle deswells with pressure to a deswollen size of $a_0 = 60$ nm.

linearity no longer holds. Overall, as expected for a system with a LCST, χ increases with increasing temperature.

Pressure-Induced Volume Transition. While the dependence of the mixing parameter of microgel particles with temperature or salt has been previously described in the literature,^{47,58,64} its dependence with hydrostatic pressure, P , has not been investigated so far. In order to obtain how χ depends on hydrostatic pressure, we measure the particle size as a function of P , at a temperature of $T = 298$ K. The application of external pressure induces a deswelling, which is closely comparable to that induced with temperature, as shown in Figure 3; the radius changes from ~ 130 nm at $P = 0.1$ MPa, to ~ 60 nm for $P > 400$ MPa. The resultant size range agrees with the size range obtained with temperature, indicative of the similar role played by pressure and temperature; both decrease the miscibility of the polymer in the solvent. In the pressure case, however, the volume transition is smoother, extending over a large pressure range.

On the basis of the size dependence with pressure and temperature, using the $\chi = \chi(T)$ relationship [Figure 2b], we can associate a mixing parameter χ to each pressure; we do this by associating the χ obtained for a certain size from the temperature measurements to the corresponding size obtained at a certain pressure. From Figure 2b and Figure 3, we thus determine the χ -dependence with pressure, as shown in Figure 4a. We find that the Flory parameter grows with external pressure following an approximately linear trend. By doing a linear fit, we obtain

$$\chi = \chi_0' + \chi_1' P \quad (8)$$

with $\chi_0' = 9.32 \times 10^{-2}$ and $\chi_1' = 2.29 \times 10^{-3}$ 1/MPa.

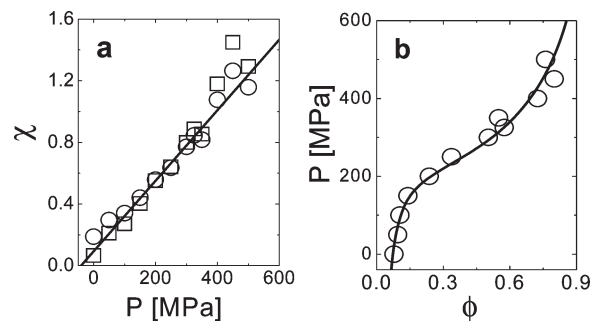


Figure 4. (a) Dependence of the Flory solvency parameter on hydrostatic pressure. The two sets of points are obtained using $\phi_0 = 0.8$ (circles) or $\phi_0 = 0.85$ (squares). (b) Pressure-induced volume transition of the pNIPAM-allylamine microgel particles in D₂O. The solid line shows the best fit according to eq 9, for $\phi_0 = 0.8$ and $N_c = 1.75 \times 10^5$.

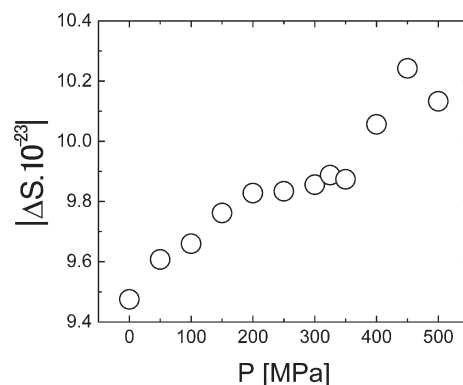


Figure 5. Absolute value of the change in the mixing entropy as a function of pressure; it increases with pressure, indicating that solvent-solvent contacts are favored over polymer-solvent contacts, which is consistent with the observed deswelling of the particles.

Assuming this result, we can write an equation of state for the pressure experiments simply by introducing eq 8 into the equilibrium condition (eq 4):

$$P = \frac{\frac{v_s N_c}{N_a V_0} \left[\left(\frac{\phi}{2\phi_0} \right) - \left(\frac{\phi}{\phi_0} \right)^{1/3} \right] - \phi - \ln(1 - \phi) - \chi_0'}{\chi_1' \phi^2} \quad (9)$$

We use this equation to fit our data, using the ϕ_0 and N_c values previously obtained from the temperature experiments, leaving χ_0' and χ_1' as free parameters. The result is shown in Figure 4b and corresponds to $\chi_0' = 9.30 \times 10^{-2}$ and $\chi_1' = 2.30 \times 10^{-3}$ 1/MPa, which are in agreement with those that resulted from the linear fit of χ versus P (Figure 4a), as expected. Furthermore, from eqs 6 and 8, it follows that at room temperature and low pressures

$$\chi_0' \approx [\chi_0 + \chi_1 \phi]_{T=298\text{K}} \quad (10)$$

Consistent with this expectation and supportive of the consistency of our data, we find that $\chi_0 + \chi_1 \phi = 0.088$, which is close to $\chi_0' = 0.093$, where we have used that at room temperature and low pressure, $\phi = 0.079$ ($a = 130$ nm).

To inquire about the χ - P relationship, we equate the Flory parameters given by eqs 6 and 8 and hypothesize that the observed change in χ with P is related to the entropic change when a solvent-solvent contact is replaced by a polymer-solvent contact, since the enthalpic change associated to this process does not appreciably depend

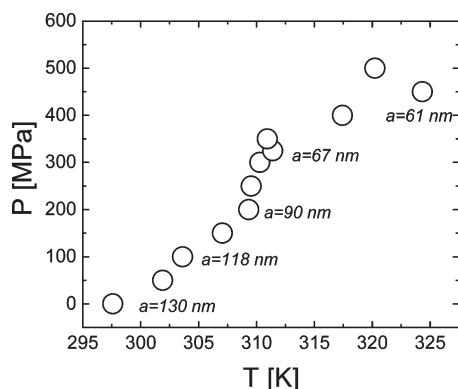


Figure 6. Pressure and temperature corresponding to the same particle size.

on external pressure.⁴⁵ We thus determine the entropy change using:

$$\Delta S = - \frac{[\chi(P) - \chi_1 \phi] k_b T - \Delta H}{T} \quad (11)$$

We find that the absolute value of the entropy change, $|\Delta S|$, increases with pressure, as shown in Figure 5; the entropy associated with a solvent–solvent contact is larger than the entropy associated to a polymer–solvent contact, ultimately causing the deswelling of the microgel particle, as we observe experimentally. Similar behavior has been previously measured for other systems which deswell with temperature^{46,63,65} or ionic concentration;⁴⁷ the absolute value of the entropy change increases as the variable triggering the deswelling increases, consistent with our data and thus supporting our hypothesis.

To finally characterize the role of hydrostatic pressure, we compare it with the role of temperature by identifying (T , P) pairs that correspond to the same particle size, as shown in Figure 6. We find that, at low pressures and temperatures, there is an approximately linear relationship between these variables indicating that both magnitudes have a similar effect on the microgel size. However, at intermediate values of pressure and temperature, a slight increase in temperature, from ~ 309 to ~ 312 K, requires a much larger increase in pressure, from ~ 200 to ~ 400 MPa, in order to change the microgel size by equal amounts. Particle deswelling thus proceeds slower when using pressure than it does when using temperature, suggesting that pressure may be a better external variable when precise tuning of the particle size and thus of the suspension volume fraction is desired.

Conclusions

We have shown that hydrostatic pressure is an effective means to deswell poly(*N*-isopropylacrylamide) microgel particles. Increasing the external pressure decreases the mixing of the polymer with the solvent causing the observed decrease in particle size; this decrease is more gradual when compared to the deswelling caused by temperature. By comparing the two, we have determined how the Flory solvency parameter depends on hydrostatic pressure; it increases with P , which we attribute to an increase in the absolute value of the entropy change when polymer–solvent contacts are replaced by solvent–solvent contacts, consistent with deswelling experiments with other polymer and gel systems. Our results open the way to use hydrostatic pressure to tune the microgel size and thus the suspension volume fraction with high precision; this could be exploited for fundamental studies where microgels are used as

colloidal particles of tunable size. In addition, understanding how pressure affects the particle size might lead to a better use of microgels in oil recovery applications,^{28–30} where these particles are subjected to pressure changes.

Acknowledgment. J.J.L.-S., B.S.-M., and A.F.-N. gratefully acknowledge FQM-03116. U.G. acknowledges financial support from the Adolphe Merkle Foundation. We acknowledge the Paul Scherrer Institute, (Villigen, Switzerland), where we performed the light scattering experiments under hydrostatic pressure.

References and Notes

- (1) Dusek, K. *Responsive Gels: Volume Transitions I*; Advances in Polymer Science Vol. 109; Springer Verlag: Berlin, 1993.
- (2) Rubinstein, M.; Colby, R. H. *Polymer Physics*; Oxford University Press: New York, 2003.
- (3) Flory, P. J. *Principles of Polymer Chemistry*; Cornell University Press: London, 1953.
- (4) Tanaka, T. *Phys. Rev. Lett.* **1978**, *40*, 820–823.
- (5) Tanaka, T.; Sato, E.; Hirokawa, Y.; Hirotsu, S.; Peetermans, J. *Phys. Rev. Lett.* **1985**, *55*, 2455–2458.
- (6) Tanaka, T.; Fillmore, D. J. *J. Chem. Phys.* **1979**, *70*, 1214–1218.
- (7) Li, Y.; Tanaka, T. *J. Chem. Phys.* **1990**, *92*, 1365–1371.
- (8) Yoshida, R.; Uchida, K.; Kaneko, Y.; Sakai, K.; Kikuchi, A.; Sakurai, Y.; Okano, T. *Nature* **1995**, *374* (6519), 240–242.
- (9) Kaneko, Y.; Sakai, K.; Kikuchi, A.; Sakurai, Y.; Okano, T. *Macromol. Symp.* **1996**, *109*, 41–53.
- (10) Matsuura, T.; Sugiyama, M.; Annaka, M.; Hara, Y.; Okano, T. *Polymer* **2003**, *44*, 4405–4409.
- (11) Yan, H.; Fujiwara, H.; Sasaki, K.; Tsujii, K. *Angew. Chem., Int. Ed.* **2005**, *44*, 1951–1954.
- (12) Noguchi, Y.; Okeyoshi, K.; Yoshida, R. *Macromol. Rapid Commun.* **2005**, *26*, 1913–1917.
- (13) Saunders, B. R.; Vincent, B. *Adv. Colloid Interface Sci.* **1999**, *80* (1), 1–25.
- (14) Pelton, R. *Adv. Colloid Interface Sci.* **2000**, *85* (1), 1–33.
- (15) Loxley, A.; Vincent, B. *Colloid Polym. Sci.* **1997**, *275*, 1108–1114.
- (16) Suarez, I. J.; Fernandez-Nieves, A.; Marquez, M. *J. Phys. Chem. B* **2006**, *110*, 25729–25733.
- (17) Pelton, R. H.; Chibante, P. *Colloids Surf.* **1986**, *20*, 247–256.
- (18) Nayak, S.; Lyon, L. A. *Angew. Chem., Int. Ed.* **2005**, *44*, 7686–7708.
- (19) Das, M.; Zhang, H.; Kumacheva, E. *Annu. Rev. Mater. Res.* **2006**, *36*, 117–142.
- (20) Fernandez-Barbero, A.; Suarez, I. J.; Sierra-Martin, B.; Fernandez-Nieves, A.; de las Nieves, F. J.; Marquez, M.; Rubio-Retama, J.; Lopez-Cabarcos, E. *Adv. Colloid Interface Sci.* **2009**, *147–48*, 88–108.
- (21) Kajiwar, K.; Rossmurphy, S. B. *Nature* **1992**, *355* (6357), 208–209.
- (22) Siepmann, J.; Peppas, N. A. *Adv. Drug Delivery Rev.* **2001**, *48* (2–3), 139–157.
- (23) Vinogradov, S. V.; Bronich, T. K.; Kabanov, A. V. *Adv. Drug Delivery Rev.* **2002**, *54* (1), 135–147.
- (24) Gao, J.; Hu, Z. B. *Langmuir* **2002**, *18*, 1360–1367.
- (25) Wagers, A. J.; Sherwood, R. I.; Christensen, J. L.; Weissman, I. L. *Science* **2002**, *297* (5590), 2256–2259.
- (26) Beebe, D. J.; Moore, J. S.; Bauer, J. M.; Yu, Q.; Liu, R. H.; Devadoss, C.; Jo, B. H. *Nature* **2000**, *404* (6778), 588–590.
- (27) Morris, G. E.; Vincent, B.; Snowden, M. J. *J. Colloid Interface Sci.* **1997**, *190* (1), 198–205.
- (28) Lamphere, J. C.; Zweigle, M. Patent US4172066 **1979**.
- (29) Chauveteau, G.; Kohler, N. *Soc. Pet. Eng. J.* **1984**, *24*, 361–368.
- (30) Snowden, M. J.; Vincent, B.; Morgan, J. C. Patent GB 226 2117A **1993**.
- (31) Debord, J. D.; Eustis, S.; Debord, S. B.; Lofye, M. T.; Lyon, L. A. *Adv. Mater.* **2002**, *14*, 658–662.
- (32) Alsayed, A. M.; Islam, M. F.; Zhang, J.; Collings, P. J.; Yodh, A. G. *Science* **2005**, *309* (5738), 1207–1210.
- (33) Bartsch, E.; Frenz, V.; Baschnagel, J.; Scharl, W.; Sillescu, H. *J. Chem. Phys.* **1997**, *106*, 3743–3756.
- (34) Purnomo, E. H.; van den Ende, D.; Vanapalli, S. A.; Mugele, F. *Phys. Rev. Lett.* **2008**, *101*, 4.
- (35) Han, Y. L.; Shokef, Y.; Alsayed, A. M.; Yunker, P.; Lubensky, T. C.; Yodh, A. G. *Nature* **2008**, *456* (7224), 898–903.
- (36) Kratz, K.; Hellweg, T.; Eimer, W. *Polymer* **2001**, *42*, 6631–6639.

- (37) Sierra-Martin, B.; Romero-Cano, M. S.; Fernandez-Nieves, A.; Fernandez-Barbero, A. *Langmuir* **2006**, *22*, 3586–3590.
- (38) Hoare, T.; Pelton, R. J. *J. Phys. Chem. B* **2007**, *111*, 1334–1342.
- (39) Nakamoto, C.; Kitada, T.; Kato, E. *Polym. Gels Networks* **1996**, *4* (1), 17–31.
- (40) Kato, E. *J. Chem. Phys.* **1997**, *106*, 3792–3797.
- (41) Kato, E. *J. Chem. Phys.* **2000**, *113*, 1310–1314.
- (42) Nakamoto, C.; Motonaga, T.; Shibayama, M. *Macromolecules* **2001**, *34*, 911–917.
- (43) Shibayama, M.; Isono, K.; Okabe, S.; Karino, T.; Nagao, M. *Macromolecules* **2004**, *37*, 2909–2918.
- (44) Kohlbrecher, J.; Bollhalder, A.; Vavrin, R.; Meier, G. *Rev. Sci. Instrum.* **2007**, *78*, 6.
- (45) Janssen, S.; Schwahn, D.; Mortensen, K.; Springer, T. *Macromolecules* **1993**, *26*, 5587–5591.
- (46) Pinkrah, V. T.; Beezer, A. E.; Chowdhry, B. Z.; Gracia, L. H.; Cornelius, V. J.; Mitchell, J. C.; Castro-Lopez, V.; Snowden, M. J. *Colloids Surf. A: Physicochem. Eng. Aspects* **2005**, *262* (1–3), 76–80.
- (47) Lopez-Leon, T.; Fernandez-Nieves, A. *Phys. Rev. E* **2007**, *75*, 011801.
- (48) Cova, S.; Ghioni, M.; Lotito, A.; Rech, I.; Zappa, F. *J. Modern Opt.* **2004**, *51*, 1267–1288.
- (49) Berne, B. J.; Pecora, R. *Dynamic Light scattering*, John Wiley: New York, 1975.
- (50) Huang, G.; Hu, Z. B. *Macromolecules* **2007**, *40*, 3749–3756.
- (51) Crea, F.; Crea, P.; De Stefano, C.; Giuffre, O.; Pettignano, A.; Sammartano, S. *J. Chem. Eng. Data* **2004**, *49*, 658–663.
- (52) Kim, J. W.; Utada, A. S.; Fernandez-Nieves, A.; Hu, Z. B.; Weitz, D. A. *Angew. Chem., Int. Ed.* **2007**, *46*, 1819–1822.
- (53) McPhee, W.; Tam, K. C.; Pelton, R. J. *Colloid Interface Sci.* **1993**, *156* (1), 24–30.
- (54) Boutris, C.; Chatzi, E. G.; Kiparissides, C. *Polymer* **1997**, *38*, 2567–2570.
- (55) Varga, I.; Gilanyi, T.; Meszaros, R.; Filipcsei, G.; Zrinyi, M. *J. Phys. Chem. B* **2001**, *105*, 9071–9076.
- (56) Sierra-Martin, B.; Choi, Y.; Romero-Cano, M. S.; Cosgrove, T.; Vincent, B.; Fernandez-Barbero, A. *Macromolecules* **2005**, *38*, 10782–10787.
- (57) Shibayama, M.; Tanaka, T.; Han, C. C. *J. Chem. Phys.* **1992**, *97*, 6829–6841.
- (58) Fernandez-Barbero, A.; Fernandez-Nieves, A.; Grillo, I.; Lopez-Cabarcos, E. *Phys. Rev. E* **2002**, *66*, 011801.
- (59) Saunders, B. R. *Langmuir* **2004**, *20*, 3925–3932.
- (60) Hirotsu, S. *Phase Transitions* **1994**, *47* (3–4), 125–125.
- (61) De Gennes, P. G. *Scaling Concepts in Polymer Physics*; Cornell University Press: Ithaca, NY, 1979.
- (62) Press, W. H.; Teukolsky, S. A.; Vetterling, W. T.; Flannery, B. P. *Numerical recipes in C: The art of scientific computing*; Cambridge University Press: Cambridge, U.K., 2002.
- (63) Pinkrah, V. T.; Beezer, A. E.; Chowdhry, B. Z.; Gracia, L. H.; Mitchell, J. C.; Snowden, M. J. *Langmuir* **2004**, *20*, 8531–8536.
- (64) Capriles-Gonzalez, D.; Sierra-Martin, B.; Fernandez-Nieves, A.; Fernandez-Barbero, A. *J. Phys. Chem. B* **2008**, *112*, 12195–12200.
- (65) Grinberg, V. Y.; Dubovik, A. S.; Kuznetsov, D. V.; Grinberg, N. V.; Grosberg, A. Y.; Tanaka, T. *Macromolecules* **2000**, *33*, 8685–8692.